

Article

## Pollutant Flux Estimation in an Estuary Comparison between Model and Field Measurements

Yen-Chang Chen <sup>1,†</sup>, Wu-Seng Lung <sup>2,†</sup>, Han-Chung Yang <sup>3,\*</sup>, Bo-Jhih Chen <sup>1,†</sup>  
and Chien-Hung Chen <sup>4,†</sup>

<sup>1</sup> Department of Civil Engineering, National Taipei University of Technology, Taipei 10608, Taiwan; E-Mails: yenchen@ntut.edu.tw (Y.-C.C.); R123628976@wracoc.wca.gov.tw (B.-J.C.)

<sup>2</sup> Department of Civil and Environmental Engineering, University of Virginia, Charlottesville, VA 22901, USA; E-Mail: wl@virginia.edu

<sup>3</sup> Department of Leisure and Tourism Management, Shu-Te University, Kaohsiung 82445, Taiwan

<sup>4</sup> Taiwan Branch, MWH Americas Inc., Taipei 10695, Taiwan; E-Mail: ricky.chen@mwhglobal.com

† These authors contributed equally to this work.

\* Author to whom correspondence should be addressed; E-Mail: hcyang@stu.edu.tw; Tel.: +886-7-615-8000 (ext. 3416); Fax: +886-7-615-8000 (ext. 3499).

*Received: 17 April 2014; in revised form: 30 July 2014 / Accepted: 15 August 2014 /*

*Published: 26 August 2014*

---

**Abstract:** This study proposes a framework for estimating pollutant flux in an estuary. An efficient method is applied to estimate the flux of pollutants in an estuary. A gauging station network in the Danshui River estuary is established to measure the data of water quality and discharge based on the efficient method. A boat mounted with an acoustic Doppler profiler (ADP) traverses the river along a preselected path that is normal to the streamflow to measure the velocities, water depths and water quality for calculating pollutant flux. To know the characteristics of the estuary and to provide the basis for the pollutant flux estimation model, data of complete tidal cycles is collected. The discharge estimation model applies the maximum velocity and water level to estimate mean velocity and cross-sectional area, respectively. Thus, the pollutant flux of the estuary can be easily computed as the product of the mean velocity, cross-sectional area and pollutant concentration. The good agreement between the observed and estimated pollutant flux of the Danshui River estuary shows that the pollutant measured by the conventional and the efficient methods are not fundamentally different. The proposed method is cost-effective

and reliable. It can be used to estimate pollutant flux in an estuary accurately and efficiently.

**Keywords:** estuary; maximum velocity; measurement; pollutant flux; water quality

---

## 1. Introduction

Field observation is invaluable to help in identifying the environmental and ecological problems in estuaries. Reliable observed pollutant flux and discharge provides the basis for theoretical analysis and modeling to help in the understanding of hydrodynamic and water quality processes. Due to global climate change, the information associated with water resources is attracting even more attention because of its importance in security and management. Thus, the pollutant flux of estuaries has become an indispensable item from the national aspect of resource administration. Establishing a long-term monitoring system for collecting the pollutant flux of estuaries is essential to provide for the applications in ecology, transportation and water resource management.

The measurement of pollutant flux in estuaries is always difficult due the following reasons: First, as the cross-section is wide and the water is deep in estuaries, it is difficult to install instruments for measuring discharges. Second, compared to the measurement of pollutant flux in non-tidal zones, there is no well-developed system to conduct long-term measurement. This explains the rare data for pollutant flux in estuaries.

Basically, a pollutant flux through an estuarine cross-section is the product of normal velocity and pollutant concentration, sectional integrated and tidally averaged [1]. It can be estimated by direct methods, which measure velocity and concentration [2,3], and indirect methods, which apply physical models [4–6]. Because of the high spatial and temporal variability in velocities and pollutant concentration [7,8], estimation of pollutant flux in an estuary by using direct methods has a long and generally discouraging history [1].

By using direct methods, discharge measurements are the key to estimate pollutant flux in estuaries. The flow in estuaries is highly unsteady, while water levels and discharges vary drastically. Discharge and concentration measurements in estuaries must be completed within a short interval. Discharge measuring in estuaries using the conventional methods is time-consuming, labor-intensive and costly. The preferred method of measuring discharge in an estuary is the moving-boat method [9,10]. Recently, the acoustic Doppler current meter (ADCP) was applied on velocity distribution measurement for estimating pollutant flux in estuaries [11,12]. Some new discharge measurement methods have been proposed to measure the discharges of estuaries to estimate pollutant flux [13–15]. However, the application of those methods on real-time measuring discharge in estuaries is yet to generate convincing results.

Discharge is not solely a function of the water level in tidally-affected areas. For a given water level, the discharge may be either large or small, and the flow direction may be either upstream or downstream. Therefore, standard stream-gauging techniques are not appropriate for estuaries [16]. To overcome these challenges, this study proposes a framework for measuring and calculating the pollutant flux. The method successfully estimates the pollutant flux in the Danshui River estuary by first determining

the relationship between the mean and maximum velocities and, then, associating the cross-sectional area with stages. Pollutant flux will be a function of cross-sectional area, cross-sectional mean velocity and pollutant concentration.

## 2. Methodology

The action of tides and tidal currents complicate estuarine processes. The water levels and flow conditions in estuaries vary temporally, and the back-and forth flow of tidal currents is the most visible feature. Therefore, the establishment of the long-term monitoring of pollutant flux in tidally-affected locations requires prompt measurement of a small amount of information and also a reliable model for accurately estimating pollutant flux from these inputs. This study applies the probabilistic velocity distribution equation for such a purpose. Pollutant concentration, stage and velocity distribution are measured directly in the field. Stage is calibrated to determine the cross-sectional area. Maximum velocity calculated from the velocity distribution is calibrated to determine the cross-sectional averaged velocity. The pollutant flux can be estimated as:

$$F_{est} = CQ_{est} = C\bar{u}_{est}A_{est} \quad (1)$$

where  $F_{est}$  is estimated pollutant flux (g/s),  $C$  is the mean pollutant concentration of the cross-section (mg/L),  $Q_{est}$  is estimated discharge (m<sup>3</sup>/s),  $\bar{u}_{est}$  is the estimated mean velocity of the cross-section (m/s) and  $A_{est}$  is the estimated cross-sectional area (m<sup>2</sup>). In the following sections, the estimation of  $\bar{u}_{est}$  and  $A_{est}$  associated with the observed parameters is provided.

### 2.1. Estimation of Cross-Sectional Mean Velocity

Chiu and Chiou [17] transformed the  $y - z$  coordinate system into the  $\xi - \eta$  coordinate system to describe the velocity distribution by a set of isovels ( $\xi$ ), which allows the relation of velocity and  $\xi$  to be one-to-one. Thus, the points on an isovel have the same velocity. Chiu utilized the  $\xi - \eta$  coordinate system on the derivation of probabilistic velocity distribution equation [18] as:

$$\frac{u}{u_{\max}} = \frac{1}{M} \ln \left[ 1 + (e^M - 1) \frac{\xi}{\xi_{\max}} \right] \quad (2)$$

where  $u$  is the velocity (m/s),  $u_{\max}$  is the maximum velocity of the cross-section (m/s),  $\xi$  is the coordinate used in a velocity distribution equation,  $\xi_{\max}$  is the value of  $\xi$  when  $u$  is the maximum velocity and  $M$  is the entropy parameter. The set of isovels  $\xi$  along the  $y$ -axis, which is the vertical section with maximum velocity in the cross-section, is:

$$\xi = \frac{y}{D-h} \exp \left( 1 - \frac{y}{D-h} \right) \quad (3)$$

where  $D$  is the water depth (m) and  $h$  is the location of the maximum velocity (m). When  $h$  is less or equal to zero, the maximum velocity occurs on the water surface, and then, Equation (2) becomes:

$$u = \frac{u_{\max}}{M} \ln \left[ 1 + \frac{y}{D} (e^M - 1) \exp \left( \frac{D-y}{D-h} \right) \right] \quad (4)$$

If  $h > 0$ , the maximum velocity occurs under the water surface  $h$ , and Equation (2) can be written as:

$$u = \frac{u_{\max}}{M} \ln \left[ 1 + \frac{y}{D-h} (e^M - 1) \exp \left( 1 - \frac{y}{D-h} \right) \right] \quad (5)$$

Therefore, Equations (4) or Equation (5) can be used to determine the maximum velocity by applying a nonlinear regression method with the observed velocity distribution.

Based upon maximizing information entropy, the method of Lagrange multipliers is applied to yield:

$$\frac{\bar{u}_{obs}}{u_{\max}} = \frac{e^M}{e^M - 1} = \Phi \quad (6)$$

where  $\bar{u}_{obs}$  is the observed cross-sectional mean velocity (m), which can be obtained as:

$$\bar{u}_{obs} = Q_{obs} / A_{obs} \quad (7)$$

where  $Q_{obs}$  and  $A_{obs}$  are the observed discharge ( $\text{m}^3/\text{s}$ ) and cross-sectional area ( $\text{m}^2$ ). This mean and maximum relation has been implemented in several areas, such as the United States [19], Italy [20], Algeria [21] and Taiwan [22], to estimate discharge in non-tidal effect streams. If the variation of natural channels is small, then the ratio of mean velocity to its maximum should be a constant [23]. Once the parameter  $\Phi$  is calibrated, the cross-sectional mean velocity can be easily determined based on Equation (6) with the cross-sectional maximum velocity.

## 2.2. Estimation of Cross-Sectional Area

The conventional approach to measure the cross-sectional area is first to divide the cross-section into several subsections and then to measure the area of each subsection. The cross-sectional area is equal to the sum of subsection areas. This approach is time-consuming. Estimating discharge in estuaries requires a fast and reliable method to determine the cross-sectional area. For a cross-section where the stream is not affected by scours and deposits, the cross-sectional area can be estimated by the stage-area relation, which was well demonstrated in the Danshui River [24], as:

$$A_{obs} = a(G - b)^d \quad (8)$$

where  $A_{obs}$  is the observed cross-sectional area ( $\text{m}^2$ ),  $G$  is the water level (m) and  $a$ ,  $b$  and  $d$  are coefficients that can be obtained by the method of nonlinear regression with the observed data. Once the parameters are determined, the cross-sectional area can be quickly calculated by Equation (8) with the water level.

## 2.3. Estimation of Pollutant Flux in Estuaries

The estimation of estuarine pollutant flux is fulfilled through the following steps. First,  $u_{\max}$  is calculated along the  $y$ -axis, and then, the mean velocity ( $\bar{u}_{est}$ ) is determined via the relation of mean and maximum velocities, as  $\bar{u}_{est} = \Phi u_{\max}$ . Then, the cross-sectional area from the stage-cross-section relation is estimated, as  $A_{est} = a(G - b)^d$ . Finally, pollutant flux is a function of pollutant concentration, area and velocity, and Equation (1) can be rewritten as:

$$F_{est} = C\Phi u_{max} a(G - b)^d \quad (9)$$

Once all of the parameters are determined, the estimation of estuarine pollutant flux becomes easy, since only the required measurements would be pollutant concentrations, stage and velocity distribution along the  $y$ -axis that enable the estimation of pollutant concentration, cross-sectional area and maximum velocity.

#### 2.4. Pollutant Flux Measurement Method

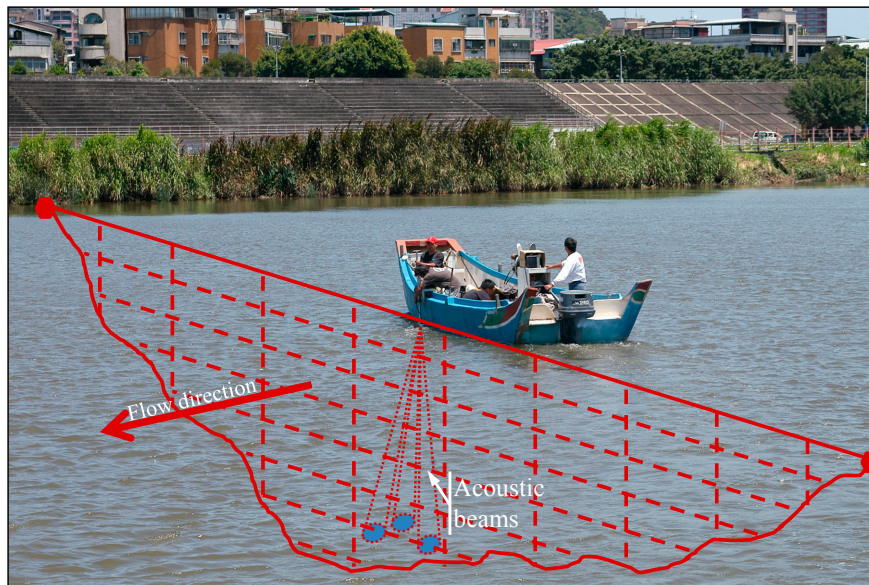
Three water samples are collected in a cross-section for determining the pollutant concentration. The sampling locations are at the 0.25, 0.5 and 0.75 channel width from the bottom and on the water surface. Therefore,

$$C = \frac{C_l + C_c + C_r}{3} \quad (10)$$

where  $C_l$ ,  $C_c$  and  $C_r$  are the pollutant concentrations (mg/L) of surface water at the 0.25, 0.5 and 0.75 channel width from the bank. The water quality data included temperature ( $^{\circ}$ C), pH (hydrogen ion concentration), electrical conductivity ( $\mu$ mho/cm), DO (dissolved oxygen, mg/L), BOD<sub>5</sub> (the biochemical oxygen demand in 5 days, mg/L), NH<sub>3</sub>-N (mg/L), chloride (mg/L), coliform group density (CFU/100 mL) and SS (suspended solids, mg/L). Once the samples are collected, they are sent to the laboratory of Société Générale de Surveillance (SGS) in Taipei. SGS follows the test methods of the Taiwan Environment Protection Agency to obtain the concentrations of pollutants.

ADP, which has been successfully demonstrated to measure discharge, is applied to collect velocity and bathymetric data. It applies the Doppler shift principle to measure velocity profiles from near the water surface to the channel bed. Not requiring the use of long strings of current meters and measuring velocity distribution in a very short time are the advantages of ADP. When conducting measurement, the transducer emits a fixed frequency sonic wave into water; as the wave hits the suspended particles in water, a frequency shift is produced due to the Doppler effect, and the echo is bounced back to the ADP, while the particle size variation also affects the intensity of the returning wave. From the property differences of emitting and returned waves, the bathymetry can be calculated; the measurement of the flow velocities can also be used to determine the profile of average flow velocity [25]. With differential global positioning system (DGPS) integration [26], the position and velocity of a vessel can be monitored to increase the accuracy of discharge measurements.

Due to the characteristics of the gauging stations, the ADPs with frequencies at 1.5 MHz and 3 MHz are used in this study. As shown in Figure 1, the vessel-mounted downward-looking ADP was used to collect the moving-boat discharge measurements. This system enables the researchers to monitor in real time the velocity and bathymetry through the laptop connected to the instruments. The vessel traverses the river along the cross-section of the gauging stations normal to the streamflow to measure discharge through continuously observing velocity, depth and position, as shown in Figure 1. This improves the spatial resolution of measurements and the ability to measure and quantify the pollutant flux in estuaries.

**Figure 1.** Schematic of the discharge measurement and bathymetric survey field method.

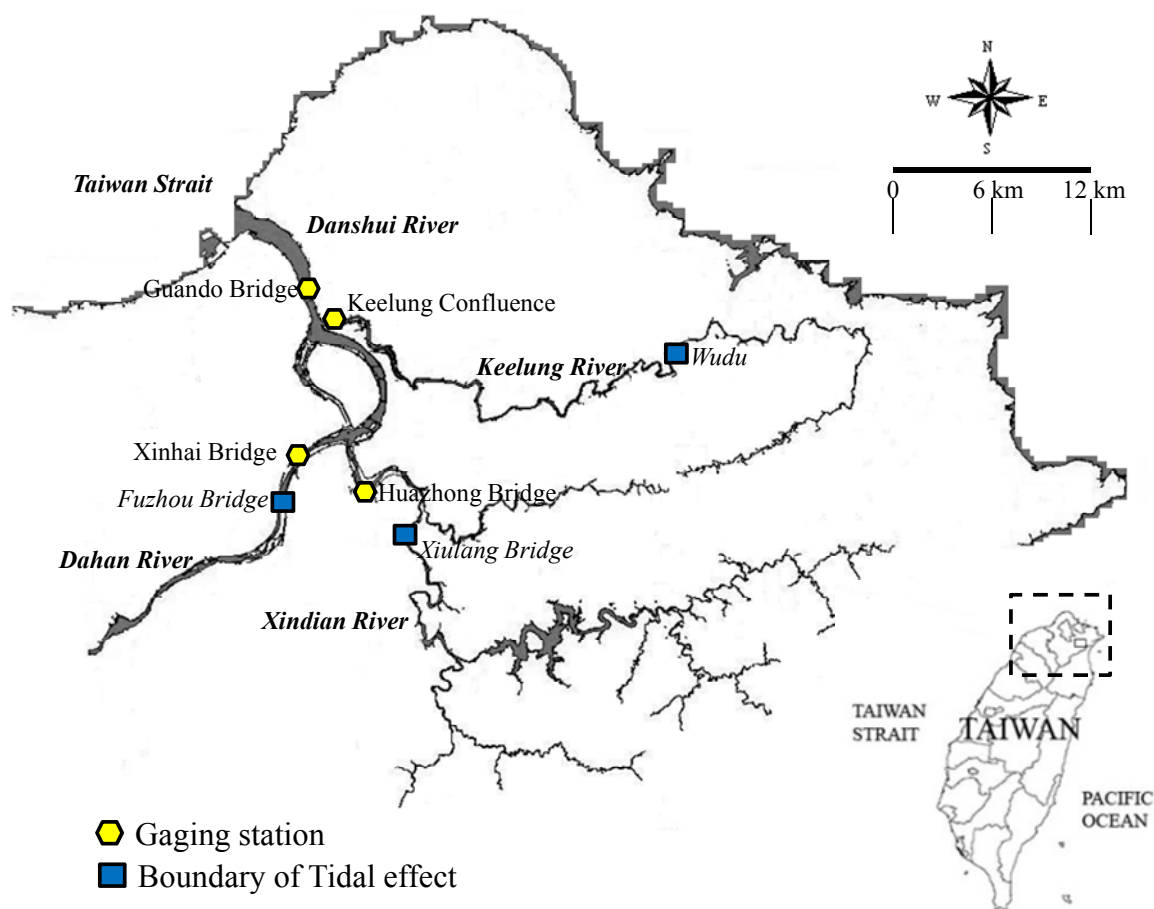
Discharge can be decomposed into small discharge contributions throughout the cross-section. Via the velocity-principle method [27], the observed pollutant flux ( $F_{obs}$ ) is calculated as:

$$F_{obs} = CQ_{obs} = C \sum v_i A_i \quad (11)$$

where  $v_i$  and  $A_i$  are the velocity and area of the grid  $i$ ., respectively. The gauge height of each gauging station is also automatically collected by the radar water level gauge.

### 3. Study Site

The Danshui River, stretching 159 km and draining a 2726-km<sup>2</sup> basin into the Taiwan Strait, is the largest estuarine system in Taiwan (see Figure 2). It flows across the Taipei metropolitan area, which has the highest population concentration in Taiwan, and is its political, economic and cultural center. Taipei is located in a low-lying basin, however, making it very susceptible to flooding; to prevent this, a flood prevention engineering project was initiated. After 1970, both raw sewage and industrial pollution from the illegal industries of the Taipei metropolitan area are discharged into the Danshui River, turning it into a heavily polluted system [28]. The restoration of the Danshui River is proposed. The goal of the project is to clean water and it includes the construction of sewer systems and wetland systems. The main stream is formed by merging three main tributaries: Dahan River, Xindian River and Keelung River; the first two with a north-south orientation converge and become the Danshui River, while the Keelung River merges in at Guando. Then, the Danshui River flows into Taiwan Strait. The main stream of the Danshui River is tidally influenced along its entire length, and parts of the tributaries are also strongly dominated by the principal lunar semidiurnal constituent ( $M_2$  tide) [29]. General studies in Taiwan indicate that the tidal stream of the Danshui River Basin can be traced back to the Keelung River at Wudu, the Dahan River at the Fuzhoa Bridge and the Xindian River at the Xiulang Bridge.

**Figure 2.** Location of the gauging station network in the Danshui River Estuary.

To evaluate the performance of restoration, four gauging stations are established to study the variations of pollutant flux in the Danshui River Estuary. The data are observed continuously for thirteen hours in order to construct a model of pollutant flux estimation. As shown in Figure 2, the stations adopted in this study include the Danshui River at the Guando Bridge, the Dahan River at the Xinhai Bridge, the Xindian River at the Huazhong Bridge and the Keelung River at the Keelung Confluence. These four gauging stations provide the data that cover the pollutant flux variation in all segments of the Danshui River Estuary and, thus, form a restoration monitoring network of the tidal zone. The choice of four gauging stations is based on the stability of the channel bed, which would provide consistent measurements, as it does not vary significantly due to hydraulic factors, such as tides, storms and floods. With this consideration, the following analysis of pollution concentration, water levels, velocity and cross-sectional area and the relationship determined would have better precision and higher reliability.

#### 4. Field Measurements

To enhance the understanding of the tidal effect on the pollutant flux in the Danshui River Estuary, a series of detailed pollutant flux measurements was made at the gauging station network from September 2009, to May 2010. Twelve sets of observation were conducted on 24 September 2009, 19 October 2009, 5 November 2009, 19 November 2009, 3 December 2009, 24 December 2009, 13 January 2010, 27 January 2010, 24 February 2010, 18 March 2010, 20 April 2010, and

4 May 2010. For each set, hourly data, including pollutant concentrations, velocities, bathymetries and stage, are collected over a complete tidal cycle. Therefore, each set includes 13 runs of observation, and 156 pollutant fluxes are computed for each gauging station. Table 1 shows the descriptive statistics of the observed data in the gauging station network. The positive values mean fluxes for flood flow, while the negative values represent ebb flow.

**Table 1.** Descriptive statistics of the water quality analysis results for each station. DO, dissolved oxygen; BOD<sub>5</sub>, the biochemical oxygen demand in 5 days; SS, suspended solids; Q<sub>obs</sub>, observed discharge; G, water level.

Station	Xinhai Bridge				Huazhong Bridge			
	Max	Min	Mean	SD	Max	Min	Mean	SD
Temperature (°C)	30.0	14.5	21.0	3.8	29.5	14.6	20.8	3.6
pH	8.19	6.50	7.19	0.24	7.77	6.88	7.18	0.17
Cond. (mho/cm)	2,220	202	611	343	4,940	87	603	809
DO (mg/L)	4.90	0.80	2.08	0.86	4.10	0.90	2.78	0.79
BOD <sub>5</sub> (mg/L)	67.8	1.7	12.2	7.7	25.4	0.5	7.9	6.0
NH <sub>3</sub> -N (mg/L)	10.5	0.0	6.3	2.4	10.2	0.0	4.5	2.6
SS (mg/L)	189.0	10.0	32.7	25.5	80.4	5.5	25.8	16.2
Cl <sup>-</sup> (mg/L)	557	15	90	97	1,620	6	155	280
<i>E. coli</i> (CFU/100 mL)	9,100,000	2,800	436,728	813,027	1,100,000	1,300	222,375	258,211
Q <sub>obs</sub> (m <sup>3</sup> /s)	288	-284	24	132	352	-291	38	142
G (m)	1.92	-0.97	0.26	0.76	7.82	3.83	5.89	0.88
A <sub>est</sub> (m <sup>2</sup> )	830	243	507	142	729	238	479	125

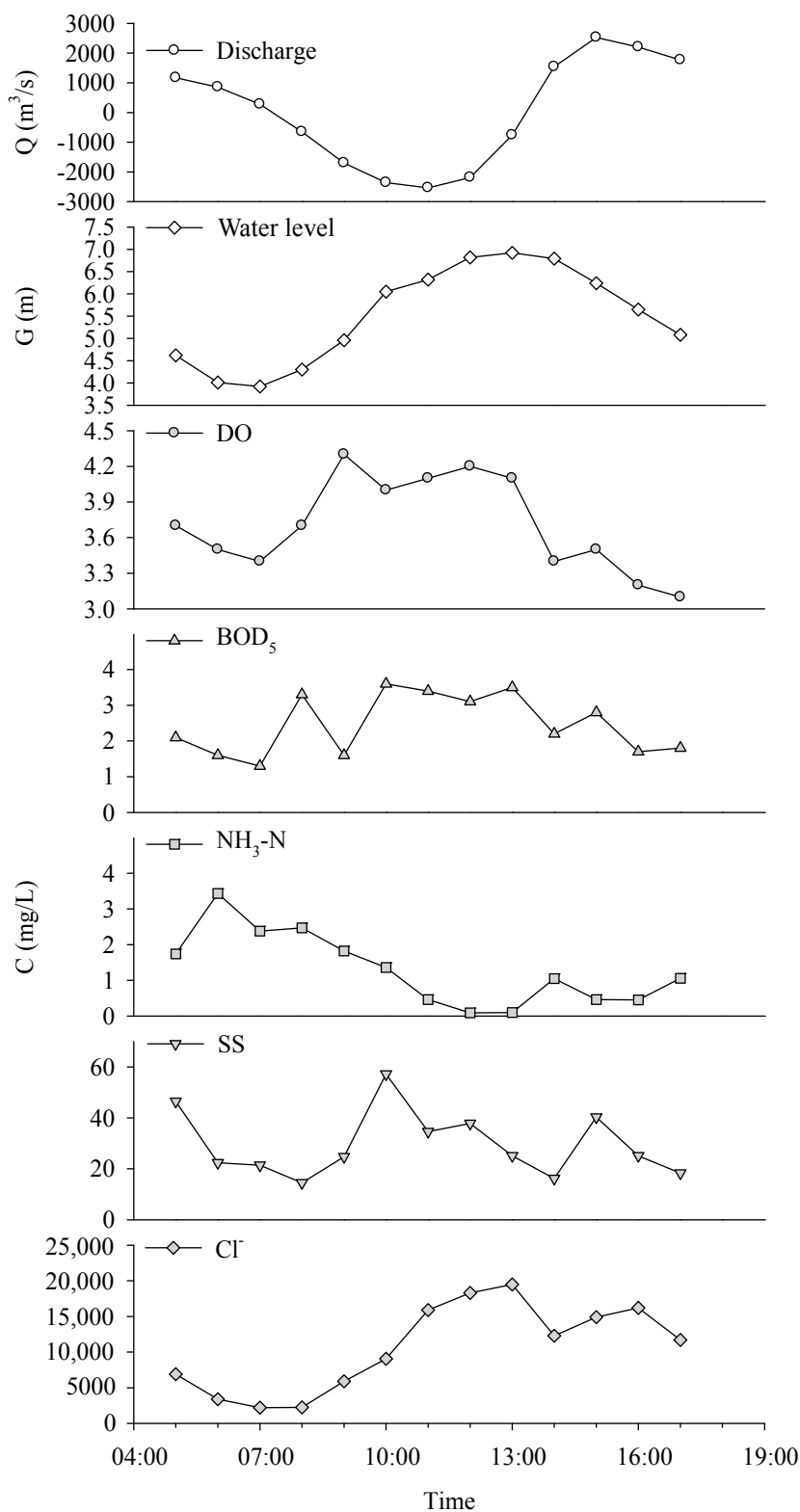
Station	Keelung Confluence				Guandu Bridge			
	Max	Min	Mean	SD	Max	Min	Mean	SD
Temperature (°C)	30.2	14.4	20.8	3.7	30.1	15.0	21.0	3.6
pH	7.98	6.23	7.12	0.28	8.18	6.41	7.39	0.37
Cond. (µmho/cm)	65,700	140	11,913	11,708	47,400	490	20,661	12,633
DO (mg/L)	5.00	0.80	2.93	0.89	5.50	1.00	3.24	0.95
BOD <sub>5</sub> (mg/L)	18.0	0.5	3.5	2.9	7.6	0.5	3.0	1.3
NH <sub>3</sub> -N (mg/L)	5.3	0.3	2.6	1.3	6.2	0.1	2.3	1.3
SS (mg/L)	102.0	6.0	23.3	17.8	138.0	6.4	22.5	17.7
Cl <sup>-</sup> (mg/L)	49,000	16	4,365	5,238	44,860	97	7,918	5,881
<i>E. coli</i> (CFU/100 mL)	790,000	10	43,364	81,160	890,000	120	39,398	87,936
Q <sub>obs</sub> (m <sup>3</sup> /s)	526	-499	28	278	2,868	-2,626	68	1,486
G (m)	1.62	-1.43	0.06	0.80	7.46	4.07	5.78	0.76
A <sub>est</sub> (m <sup>2</sup> )	1,019	317	671	176	3,578	1,923	2,776	380

The periodic tidal phenomena strongly affect the estuarine flow rates and stage levels. The flood discharge usually increases during flood tide and then decreases until slack water occurs about two hours after the high water level. Then, the discharge falls as the tide ebbs and the current again reaches a maximum. Approximately four hours after low water level, there is again slack water, with generally a high and low slack tide each tidal cycle. The pollutant concentrations measured simultaneously are shown in Figure 3. The concentrations of BOD<sub>5</sub>, DO, SS, NH<sub>3</sub>-N and Cl<sup>-</sup> fluctuate according to the water levels. The maximum and minimum concentrations of BOD<sub>5</sub>, DO, SS and Cl<sup>-</sup> and the high water



level and low water level are almost out of phase. Contrarily, the maximum and minimum concentrations of  $\text{NH}_3\text{-N}$  occur at the low water level and high water level.

**Figure 3.** Pollutant concentrations, water stage and discharge measured over a complete tidal cycle at Guando Bridge.



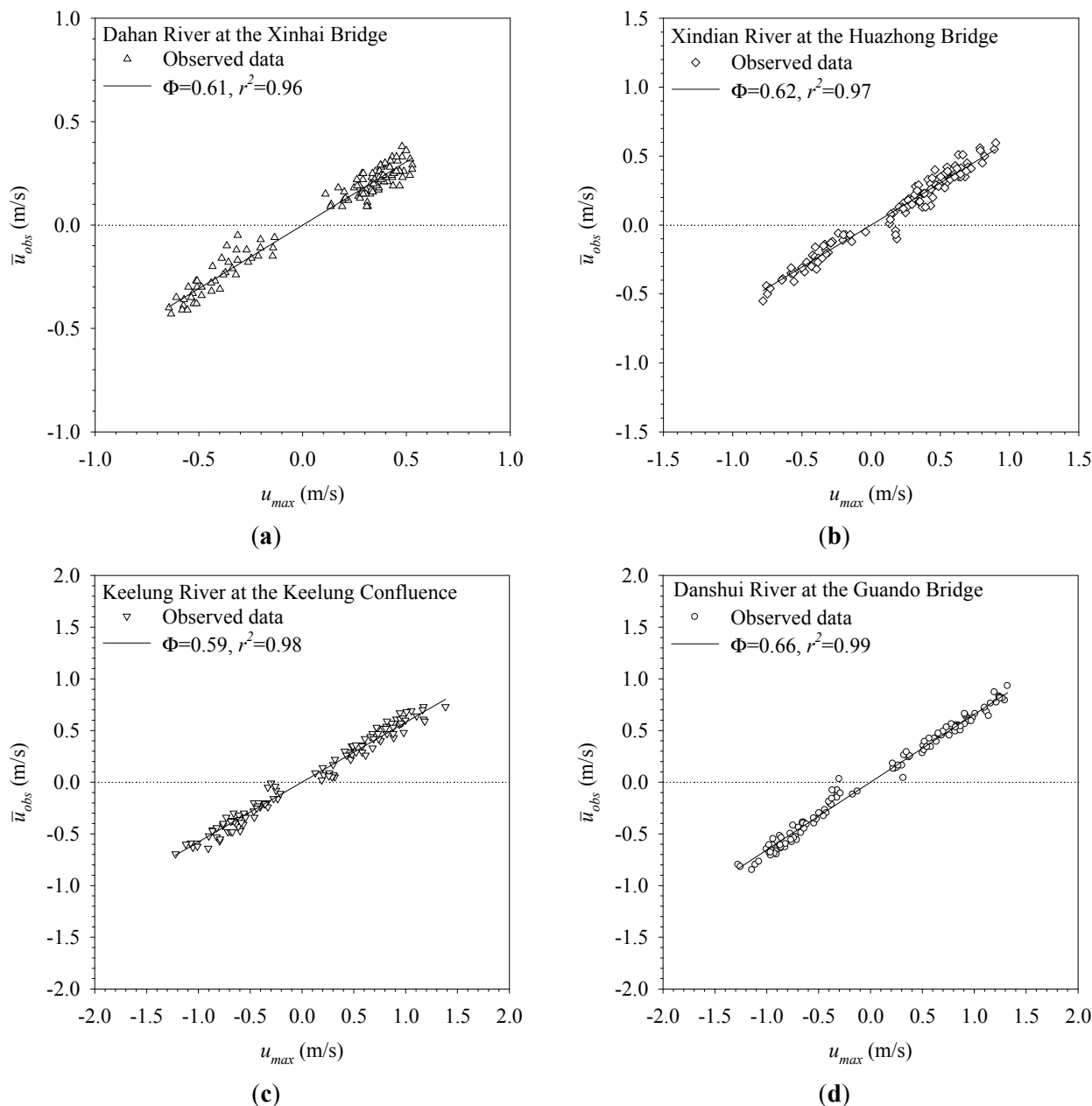
## 5. Results

The observed data is separated into a calibration subset and a validation subset. The calibration subset, the first nine datasets (24 September 2009–24 February 2010), is used to determine the parameters of the method of pollutant flux estimation. The validation set, the data collected on 18 March 2010, 20 April 2010, and 4 May 2010, are applied to show the performance of this method. Thus, the validation subset data are not used to derive and determine the parameters of the method.

The velocity used for calculating the discharge that can be used to plot the isovels in the cross-section reveals the location of maximum velocity. The  $y$ -axis ( $Z_y$ ), which is the vertical maximum velocity that occurs, is very stable and invariant with time, discharge and gauge height if the channel bed does not change drastically. A slight shift of the  $y$ -axis will not have much effect on the maximum velocity [9]. Therefore,  $u_{max}$  can be calculated based on the velocity distribution at the mean location of the  $y$ -axis ( $\bar{Z}_y$ ). The results obtained at different discharges and water levels indicate that  $\bar{Z}_y$  of the Xinhai Bridge, whose channel width is about 520 m, is 61.90 m from the left bank with a standard deviation of 12.02 m. This and other similar results from the other gauging stations show that  $\bar{Z}_y$  does not have a trend varying with time and discharge, although they show some fluctuations around the mean. This demonstrates the stability of the  $y$ -axis, even under the different flow conditions of the gauging stations. Thus,  $u_{max}$  can be estimated at  $\bar{Z}_y$  for each of the four gauging stations. To estimate the maximum velocity, the vertical velocity distribution sampled on  $\bar{Z}_y$  can be used. Based on the detailed velocity distribution,  $u_{max}$  can be determined along with  $M$  and  $h$  by nonlinear regression using Equation (4) or Equation (5).

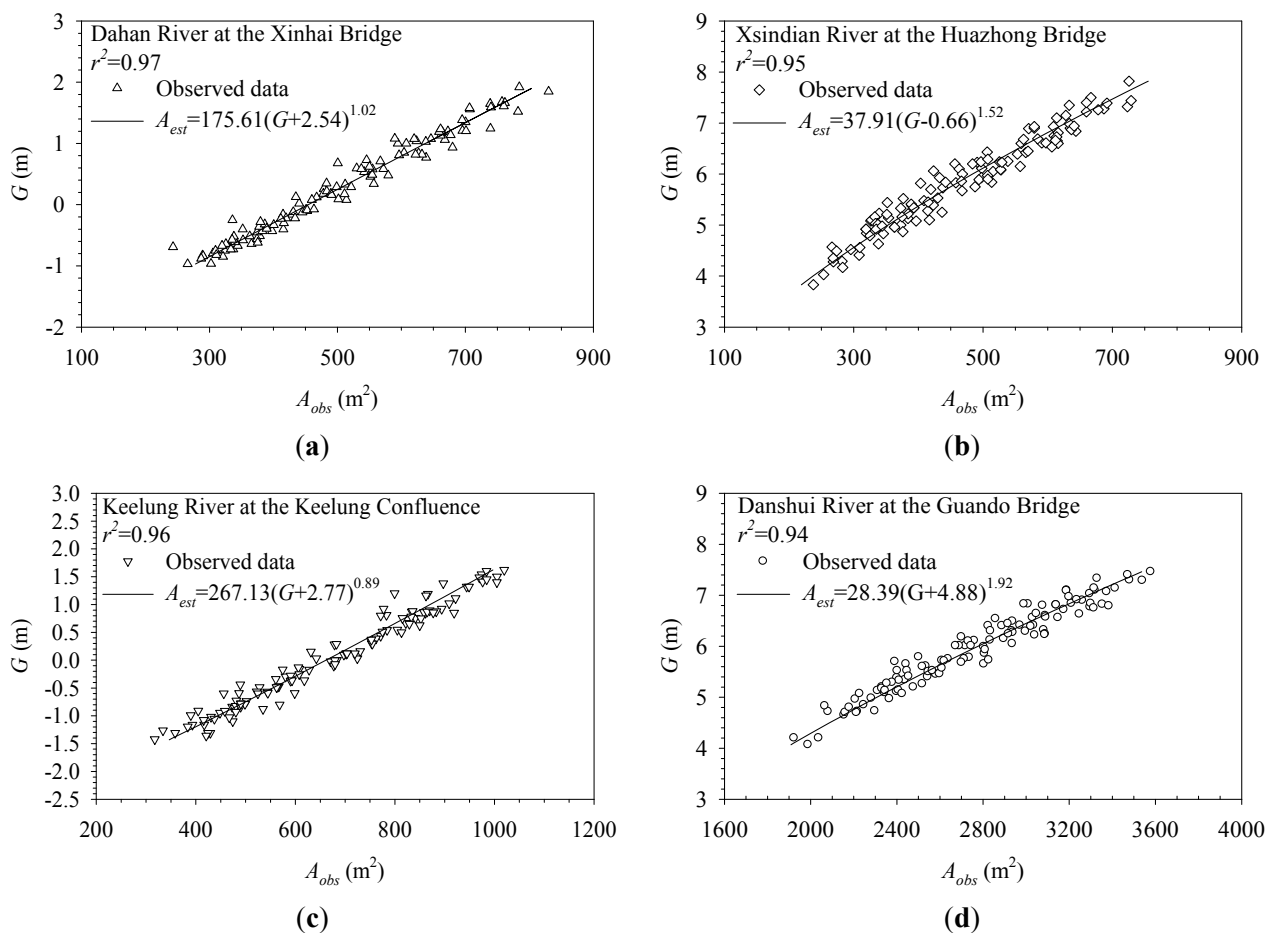
Based on the data of the calibration subset, Figure 4 presents the relations between the mean and maximum velocities with a large correlation coefficient (close to one) at the four gauging stations. The positive and negative velocities in Figure 4 represent flow directions, downstream and upstream. Mathematically, they have a linear relationship crossing through the origin.  $\Phi$  of the Xinhai Bridge is fairly constant and stable at 0.61 during flood, slack and ebb tides and not very sensitive to a possible error in locating  $\bar{Z}_y$ . The excellent mean and maximum velocities relation indicates that  $\Phi$  will not vary with flow condition or sediment concentration. This result indicates the capability of using maximum velocity to accurately estimate mean velocity at the Xinhai Bridge. Similar results are found in the other three gauging stations.  $\Phi$  of Huazhong Bridge, Keelung Confluence and Guando Bridge are 0.62, 0.59 and 0.66, respectively.  $r^2$  of Huazhong Bridge, Keelung Confluence and Guando Bridge are also very close to one. To further examine the mean and maximum relation, the data of the validation subset are used to verify the stability of  $\Phi$ .

**Figure 4.** Relation of maximum and mean velocities in the gauging station network during the calibration phase: **(a)** Xinhai Bridge; **(b)** Huazhong Bridge; **(c)** Keelung Confluence; **(d)** Guando Bridge.



The relationship between the water level and cross-sectional area for each gauging station is shown in Figure 5. At Xinhai Bridge, Huazhong Bridge, Keelung Confluence and Guando Bridge, the cross-sectional area can be determined as  $175.61(G + 2.54)^{1.02}$ ,  $37.91(G - 0.66)^{1.52}$ ,  $167(G + 2.77)^{0.89}$  and  $28.39(G + 4.88)^{1.92}$ , respectively. It can be seen that the rating curves are very close to the scatter data. No significant deviation is observed. The results show that the stage-area rating curve is robust in estimation.

**Figure 5.** Relation of water level and cross-sectional area in the gauging station network during calibration phase: (a) Xinhai Bridge; (b) Huazhong Bridge; (c) Keelung Confluence; (d) Guando Bridge.



The performance of the proposed method can be evaluated by a comparison of observed and estimated pollutant fluxes at various locations in the Danshui River Estuary. The accuracy obtained is better visualized by Figure 6, which displays scatters plots of estimated and observed values. All points fall fairly close to the agreement line, and the value of  $r^2$  is 0.99 during calibration and validation phases. The accuracy can be quantified by the good performance of mean velocities estimated by maximum velocities and cross-sectional areas estimated by water levels. Table 2 also lists the square of the correlation coefficients (R-square,  $r^2$ ) and the root mean squared errors (RMSEs) of the methods used in this study. The units in Table 2 for the RMSEs of  $\bar{u}_{est}$ ,  $A_{est}$  and  $F_{est}$  are m/s,  $m^2$  and g/s, respectively. The reliability and accuracy of the proposed method is further supported by the statistical analysis, as the values of  $r^2$  are close to one, while the RMSEs are all relatively small. Figure 7 gives examples of the time series of pollutant flux obtained in the Danshui River Estuary from the actual measurement of pollutant flux at Guando Bridge on 4 May 2010. The dots are representative of pollutant flux; the curves are estimated by the proposed method. It shows a fair agreement between measured and estimated pollutant flux. The results indicate the capability of using mean pollutant concentration, maximum velocity and water level to reliably and accurately estimate pollutant flux in estuaries.

**Figure 6.** Accuracy and reliability of the pollutant flux estimation by using the efficient method: (a) BOD; (b) NH<sub>3</sub>-N; (c) SS; (d) Cl<sup>-</sup>.

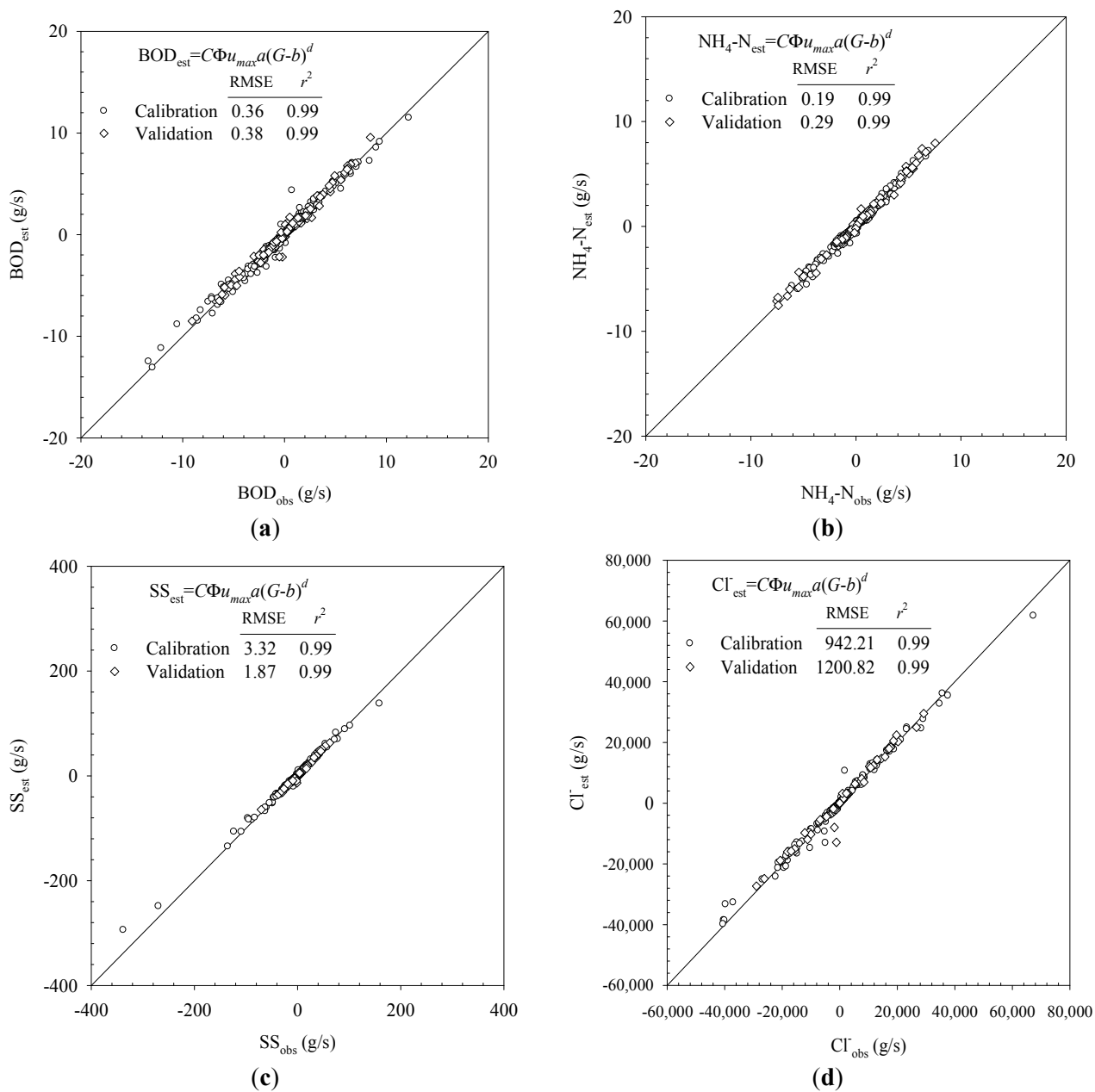
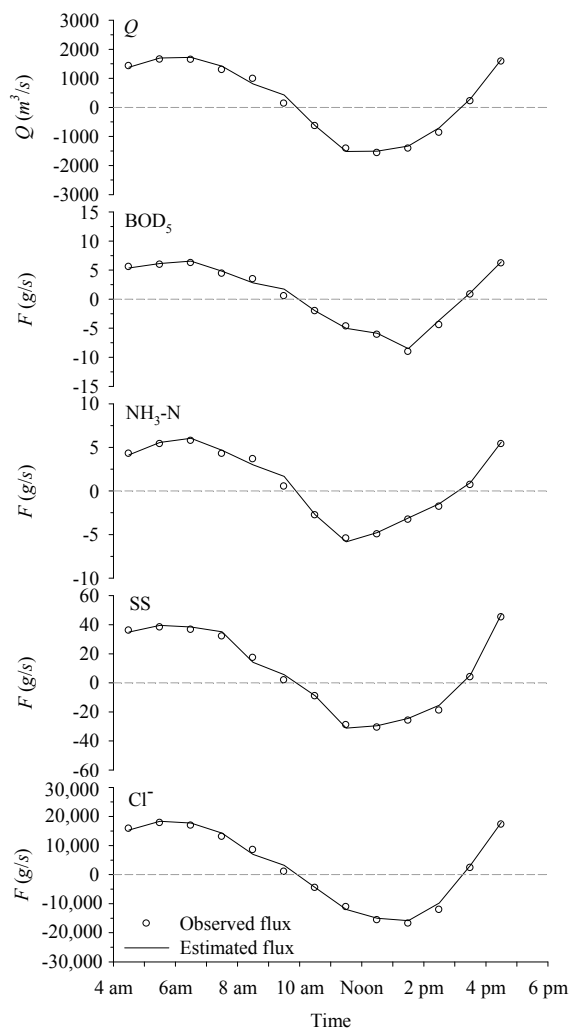


**Table 2.** Summary description of R-square ( $r^2$ ) and root mean squared error (RMSE).

Station		$r^2$ /RMSE			
		Xinhai Bridge	Huazhong Bridge	Keelung Confluence	Guandu Bridge
Calibration	$\bar{u}_{est}$	0.98/0.02	0.98/0.03	0.99/0.06	0.99/0.03
	$A_{est}$	0.98/17	0.97/20	0.98/35	0.97/55
	$F_{est}$ -BOD	0.99/0.26	0.98/0.23	0.99/0.23	0.99/0.58
	$F_{est}$ -NH <sub>3</sub> -N	0.98/0.14	0.99/0.08	0.99/0.09	0.99/0.33
	$F_{est}$ -SS	0.98/1.01	0.99/0.88	0.99/1.41	0.99/6.19
	$F_{est}$ -Cl <sup>-</sup>	0.99/3.08	0.99/1.80	0.99/387.75	0.99/1799.70
Validation	$\bar{u}_{est}$	0.98/0.04	0.98/0.05	0.99/0.07	0.99/0.06
	$A_{est}$	0.99/37	0.97/33	0.99/27	0.99/55
	$F_{est}$ -BOD	0.98/0.41	0.99/0.13	0.99/0.18	0.99/0.63
	$F_{est}$ -NH <sub>3</sub> -N	0.99/0.22	0.99/0.14	0.99/0.14	0.99/0.49
	$F_{est}$ -SS	0.98/1.16	0.99/0.48	0.99/0.61	0.99/3.50
	$F_{est}$ -Cl <sup>-</sup>	0.99/5.85	0.99/6.26	0.99/208.23	0.99/2432.13

**Figure 7.** Comparison of measured and estimated flux curves during flood, slack and ebb tides. Field observations conducted in the Danshui River Estuary at the Guando Bridge on 4 May 2010.



## 6. Conclusions

Reliably measured pollutant flux is invaluable to know the characteristics of the hydrodynamic processes and the fate and transport of pollutants in an estuary, to provide the basis for theoretical analysis and numerical modeling. Estuaries have complicated flow conditions due to the tidal effects. Due to budget, time and technological constraints, the pollutant flux data in an estuary are rarely sufficient. To overcome such constraints, a method that can estimate pollutant flux in a fast, yet simple, fashion within the tidal zones is thus needed.

The method of pollutant flux estimation modelling in estuaries can solve the problem through the following steps: first, estimating the mean pollutant concentration of the cross-section; second, to determine the mean velocity using a probabilistic velocity distribution equation; third, to estimate the cross-sectional area using the water level. Once the coefficients for the formula in the method are determined, only few data are needed to be collected to estimate the pollutant flux of estuaries. Therefore, with the proposed method, the long-term and real-time monitoring of pollutant flux in estuaries can be achieved through the installation of instruments at carefully chosen study sites.

This research studied the Danshui River estuary and established a monitoring network for the pollutant flux with state-of-the-art instruments to construct the pollutant flux estimation method. The data collected are also used to verify the applicability of the proposed method. The results demonstrate that the efficient method is able to estimate the pollutant flux in a fast, accurate and reliable fashion for the estuaries. This method furthermore reduces the time needed to conduct the pollutant flux measurement, as well as the quantity of human labor, material and risks for such a task.

## Acknowledgments

This paper is based on the work of and the financial support given by Taipei County, Taiwan.

## Author Contributions

All of the authors contributed to the manuscript. Yen-Chang Chen, Wu-Seng Lung, Han-Chung Yang, Bo-Jhih Chen and Chien-Hung Chen have contributed to the research methods, and the results have been discussed among all authors. Authorship credit is based on all of the authors having contributed to the conception and design, acquisition of data or the analysis and interpretation of data.

## Conflicts of Interest

The authors declare no conflict of interest.

## References

1. Jay, D.A.; Geyer, W.R.; Uncles, R.J.; Vallino, J.; Largier, J.; Boynton, W.R. A review of recent developments in estuarine scalar flux estimation. *Estuaries* **1997**, *20*, 262–280.
2. Aubrey, D.G.; Speer, P.E. A study of non-linear tidal propagation in shallow inlet/estuarine systems Part I: Observations. *Estuar. Coast. Shelf Sci.* **1985**, *21*, 185–205.

3. Dyer, E.R.; Gong, W.K.; Ong, J.E. The cross sectional salt balance in a tropical estuary during a lunar tide and a discharge event. *Estuar. Coast. Shelf Sci.* **1992**, *34*, 579–591.
4. Gardner, L.R.; Kjerfve, B.; Petrecca, D.M. Tidal fluxes of dissolved oxygen at the North Inlet-Winyah Bay National Estuarine Research Reserve. *Estuar. Coast. Shelf Sci.* **2006**, *67*, 450–460.
5. Ji, Z.-G. *Hydrodynamics and Water Quality: Modeling Rivers, Lakes, and Estuaries*; John Wiley & Sons: Hoboken, NJ, USA, 2007.
6. Liu, W.-C.; Huang, W.-C. Modeling the transport and distribution of fecal coliform in a tidal estuary. *Sci. Total Environ.* **2012**, *431*, 1–8.
7. Kjerfve, B.L.; Stevenson, H.; Proehl, J.A.; Chrzanowski, T.H.; Kitchens, W.M. Estimation of material fluxes in an estuarine cross section: A critical analysis of spatial measurement. *Limnol. Oceanogr.* **1981**, *26*, 325–335.
8. Ferguson, A.; Eyre, B.; Gay, J. Nutrient cycling in the sub-tropical Brunswick estuary, Australia. *Estuaries* **2004**, *27*, 1–17.
9. Rantz, S.E. *Measurement and Computation of Streamflow: Volume 1. Measurement of Stage and Discharge*; Geological Survey Water-Supply Paper 2175; US Government Printing Office: Washington, DC, USA, 1982.
10. International Organization for Standardization (ISO). *Measurement of Liquid Flow in Open Channels-Moving-Boat Method*; ISO: Geneva, Switzerland, 1979.
11. Santamarina Cuneo, P.; Flemming, B.W. Quantifying concentration and flux of suspended particulate matter through a tidal inlet of the East Frisian Wadden sea by acoustic doppler current profiling. *Proceed. Mar. Sci.* **2000**, *2*, 39–52.
12. Vaz, N.; e Silva, J.D.L.; Dias, J.M. Salt fluxes in a complex river mouth system of Portugal. *PLoS One* **2012**, *7*, e47349, doi:10.1371/journal.pone.0047349.
13. Kawanisi, K.; Razaz, M.; Kaneko, A.; Watanabe, S. Long-term measurement of stream flow and salinity in a tidal river by the use of the fluvial acoustic tomography system. *J. Hydrol.* **2010**, *380*, 74–81.
14. Hidayat, H.; Vermeulen, B.; Sassi, M.G.; Torfs, P.J.J.F.; Hoitink, A.J.F. Discharge estimation in a backwater affected meandering river. *Hydrol. Earth Syst. Sci.* **2011**, *15*, 2717–2728.
15. Bechle, A.J.; Wu, C.H.; Liu, W.-C.; Kimura, N. Development of application of an automated river-estuary discharge imaging system. *J. Hydraul. Eng.-ASCE* **2012**, *138*, 327–339.
16. Braca, G. *Stage-Discharge Relationships in Open Channels: Practices and problems, FORALPS Technical Report*; Università degli Studi di Trento: Trento, Italy, 2008.
17. Chiu, C.-L.; Chiou, J.-D. Structure of 3-D flow in rectangular open-channels. *J. Hydraul. Eng.-ASCE* **1986**, *112*, 1050–1068.
18. Chiu, C.-L. Velocity distribution in open-channel flow. *J. Hydraul. Eng.-ASCE* **1989**, *115*, 576–594.
19. Chiu, C.-L.; Chen, Y.-C. An efficient method of discharge estimation based on probability concept. *J. Hydraul. Res.* **2003**, *41*, 589–596.
20. Moramarco, T.; Saltalippi, C.; Singh, V.P. Estimation of mean velocity in natural channels based on Chiu's velocity distribution equation. *J. Hydraul. Eng.-ASCE* **2004**, *9*, 42–50.
21. Ammari, A.; Remini, B. Estimation of Algerian Rivers discharges based on Chiu's equation. *Arab. J. Geosci.* **2001**, *3*, 59–65.



22. Chen, Y.-C.; Kuo, J.-J.; Yu, S.-R.; Liao, Y.-J.; Yang, H.-C. Discharge estimation in a lined canal using information entropy. *Entropy* **2014**, *16*, 1728–1742.
23. Chiu, C.-L.; Hsu, S.-M. Probabilistic approach to modeling of velocity distributions in fluid flows. *J. Hydrol.* **2006**, *316*, 28–42.
24. Chen, Y.-C.; Chiu, C.-L. An efficient method of discharge measurement in tidal streams. *J. Hydrol.* **2002**, *265*, 212–224.
25. Yorke, T.H.; Oberg, K.A. Measuring river velocity and discharge with acoustic Doppler profilers. *Flow Meas. Instrum.* **2002**, *13*, 191–195.
26. Hofmann-Wellenhof, B.; Lichtenegger, H.; Collins, J. *Global Positioning System: Theory and Practice*; Springer-Verlag: Wien, NY, USA, 2001.
27. Herschy, R.W. *Streamflow Measurement*; Taylor & Francis: New York, NY, USA, 2009.
28. Chen, C.-H.; Lung, W.-S.; Li, S.-W.; Lin, C.-F. Technical challenges with BOD/COD modeling of river in Taiwan. *Hydro-Environ. Res.* **2012**, *6*, 3–8.
29. Chen, Y.-C.; Kao, S.-P.; Chiang, H.-W. Defining an estuary using the Hilbert-Huang Transform. *Hydrol. Sci. J.* **2013**, *58*, 841–853.

© 2014 by the authors; licensee MDPI, Basel, Switzerland. This article is an open access article distributed under the terms and conditions of the Creative Commons Attribution license (<http://creativecommons.org/licenses/by/3.0/>).